Towards 21%: front side improvements for n-Pasha solar cells

I. Romijn[1], G. Janssen[1], M. Koppes[1], J. Liu[1], Y. Komatsu[1], J. Anker[1], A. Gutjahr[1], E. Kossen, A. Mewe[1], K. Tool[1]
O. Siarheyeva[2], M. Ernst[2]
1: ECN Solar Energy, P.O. Box 1, NL-1755 ZG Petten,
2: Levitech BV, Versterkerstraat 10, NL-1322 AP Almere,
The Netherlands, Phone: +31 224 564309; Fax: +31 224 568214; email: romijn@ecn.nl

Abstract:

The purpose of the work presented in this paper is to show cost effective and industrial solutions for the tuning of boron emitters, surface preparation and passivation of n-Pasha solar cells. The n-Pasha cells now reach average efficiencies of 20.4%, with op efficiencies of 20.5%. One of the main limiting factors for n-Pasha cells currently is the boron emitter and its passivation [1]. We present a simple and effective method to tune the emitter profile such that the recombination is decreased while the sheet conductance and contact ability is largely unaffected. The boron emitter profile is tuned using a new method of etching the surface by 10-20 nm, resulting in a boron emitter without boron depletion at the surface. The emitter recombination current J_{0E} is decreased from 100 fA/cm^2 to 60 fA/cm^2 while maintaining the sheet resistance at 60 ohm/sq. n-Pasha cells made with these profiles exhibit a higher V_{oc} by 6 mV and a higher efficiency by 0.2% absolute.

Several parameters related to the surface cleaning, variations of chemical oxide passivation and dielectric layers have also been investigated. Implied V_{oc} and J_0 are determined to characterize the quality of the passivation effect, and combined with the emitter profiles in 2D Atlas simulations to estimate the improvement on the surface recombination velocity SRV. We found that a very high implied V_{oc} of 680±2 mV can be obtained with an improved pre-cleaning followed by a wet chemical surface oxidation and ALD Al_2O_3 capped with PECVD-SiN_x. The associated values for SRV are reduced from above 10^4 cm/s towards 1000 cm/s.

Combining the improved emitter profile and the improved surface passivation, values of J_{0E} of 40 – 50 fA/cm^2 for contactable boron emitters are within reach. Implementation of these modifications is expected to result in a large step towards efficiencies of 21%.

Keywords: bifacial, n-type cells, boron emitters, passivation

1 Introduction

Currently, majority of PV manufacturing still relies on mc-Si p-type. However, the fourth edition of the International Technology Roadmap for Photovoltaics [2] predicts a clear shift from p-type to n-type mono-Si within the crystalline Si market, with the share of n-type mono cells rising to over 30% in 2023. Compared to p-type material, n-type Cz material is known for its stable high carrier lifetimes because of the absence of light-induced degradation (LID) and its higher tolerance of the most common metallic impurities, such as Fe [3,4]. The highest efficiency crystalline silicon modules that are currently on the market are fabricated on n-type Cz material by the companies Sunpower, Panasonic and Yingli Solar [5-7].

1.1 n-Pasha cells

To realize high efficiencies at low cost, ECN has developed the n-Pasha solar cell concept on n-type Czochralski (Cz) base material [8,9]. The n-Pasha cell is a bifacial solar cell concept with average efficiencies of 20.2– 20.4%; and a top efficiency of 20.5% has been demonstrated. A cross section of a n-Pasha cell is shown in Figure 1.

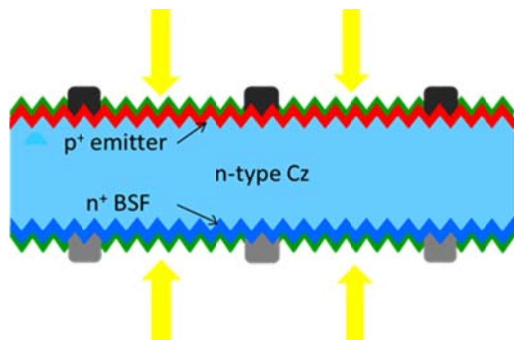

Figure 1: Cross section of the ECN n-Pasha cell. Yingli's PANDA cells are also based on this structure. It features an n-type Cz Si wafer with a boron-p+ emitter and phosphorous-n+ BSF

The n-Pasha cells are fabricated on 6 inch n-type Cz wafers, and all processing steps used for the n-Pasha cell at ECN are compatible with an industrial scale. After the wafers receive a random pyramid texture using alkaline etching, the boron emitter and phosphorous BSF are formed with a co-diffusion step using an industrial tube furnace from Tempress. A 60 Ω/sq emitter is made using BBr3 as precursor. The BSF is made using POCl3 as precursor and provides additional lateral conductivity at the rear side. This results in a good fill factor despite the open rear side metallization, even for cells processed on high resistivity base material (~10 Ωcm) [9]. In this way the BSF is an important element of the cell design providing a solution for reduced performance sensitivity towards variations in the n-type wafer resistivity [10]. Both the front and rear side are coated with SiN_x layers for passivating and anti-reflective purposes. The metal grids are printed, and the contacts on emitter and BSF are formed during a single co-firing step. Both front and rear metallization can be directly soldered so no additional metallization step is necessary to enable interconnection into a module, and the module manufacturing and costs are therefore the same as for standard p-type cells.

The symmetric structure of the open front and rear side metallization ensures that the bowing of the cells will be strongly reduced when (very) thin wafers are used, which is a distinct advantage to the bowing that occurs for full area aluminum BSFs on p-type solar cells. Furthermore, the dielectric coating on the rear side results in an improved surface passivation as compared to the conventional full area aluminum rear side of p-type cells, while the optical properties of the dielectric layer can be tuned to enable optimal (anti) reflective properties. If the cells are put in a standard mono-facial module, the refractive indices can be tuned to obtain maximum reflection in combination with the module back-sheet foil. On the other hand, the open rear side H-patterned metallization makes the n-Pasha concept very suitable for bifacial cell & module technology. This way, an even higher module output power and an increased annual energy yield can be obtained when they are placed in an appropriate way in the field. Recent results have shown that the output power of bifacial n-Pasha modules can be increased by almost 20% if the bifacial modules were placed in front of a higher reflective background [11].

1.2 ECN roadmap

In this conference ECN presents three related n-type cell technologies: n-pasha, n-MWT [12] and the recently developed n-IBC Mercury cells 13]. The n-pasha cells in general are described in the section above, and recent developments on these cells will be further discussed in the remainder of this paper.

ECN's n-type MWT cell [14] uses processing very similar to the industrial n-Pasha cells. Laser processing is used to form via-holes by which the front side metal grid is wrapped through the wafer. n-MWT modules allow an efficiency gain by combining the proven n-pasha technology with a rear contact module technology, and are industry ready.

Recently ECN has presented n-type IBC Mercury cells [15], that employ a relatively conductive Front Floating Emitter to avoid electrical shading issues in conventional FSF IBC cells, resulting in relaxed demands on the geometrical resolution in the processing. This allows processing of efficient IBC cells (no metal at the front side) with n-pasha type technology and a process complexity similar to that of n-pasha and n-MWT cells. The IBC Mercury design can be combined with ECN's back-contact technology similar to n-MWT cells.

All three n-type cell technologies aim to provide a solution towards high efficient, but low cost and easy to manufacture cells and modules.

2 Atlas simulations

2.1 Recombination current parameter J_0 as a function of surface recombination velocity

Currently, one of the main limiting factors for high efficient n-type front junction solar cells is the boron emitter, its contacting and its passivation. 2 dimensional Atlas [16] simulations are used as a guideline to monitor our progress on boron emitters and their passivation for n-type front junction solar cells. In Figure 2, electrochemical capacitance-voltage (ECV) measurements of 3 investigated boron emitter profiles are shown. Emitter profile 1 is that of a typical, 60 ohm/sq diffused boron emitter. Boron profile 2 also results in a 60 ohm/sq emitter, while profile 3 has a sheet resistivity of 85 ohm/sq. For both profile 2 and 3 the typical boron depleted region is absent.

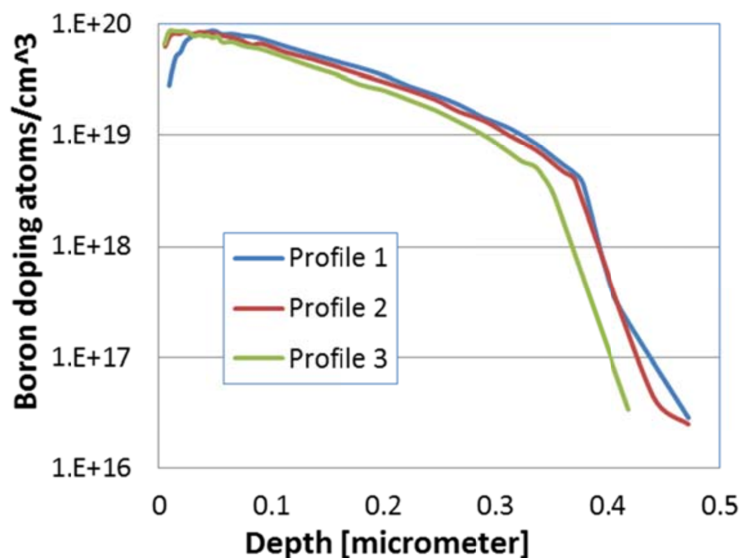

Figure 2: 3 different boron profiles as measured with ECV; Profile 1 and 2 both result in R_{sheet} of 60 ohm/sq, profile 3 has a R_{sheet} of 85 ohm/sq.

In Figure 3 values for emitter recombination current parameter J_0 as function of surface recombination velocity SRV are shown. These have been calculated using Atlas [16] for the 3 different boron profiles shown in figure 2. For low SRV's the J_0 values saturate at the Auger limit. Reducing J_{0E} is an important part of improving the cell efficiency, as V_{oc} can be expressed as:

$$V_{oc} = \frac{kT}{q} ln\left(\frac{J_l}{J_0} + 1\right) , \qquad (1)$$

where the effective J_0 is approximated by J_0=J_{0E}+J_{0BSF} + $J_{0contact}$ + J_{0bulk}.

Equation 1 implies that V_{oc} increases logarithmically with decreasing J_{0E}. As can be seen from Figure 3, J_{0E} can be reduced by improved passivation (reducing the SRV) for a specific profile. Moreover, comparing profile 1 and 2 in Figure 3 also shows that improved profiles can be implemented that reduce the effect of surface recombination on the J_{0E} , and reduce the J_{0E} by itself. Profile 2 shows a decrease in slope of the J_0(SRV) curve as compared to profile 1, without increasing of the Auger limit or the sheet resistance.

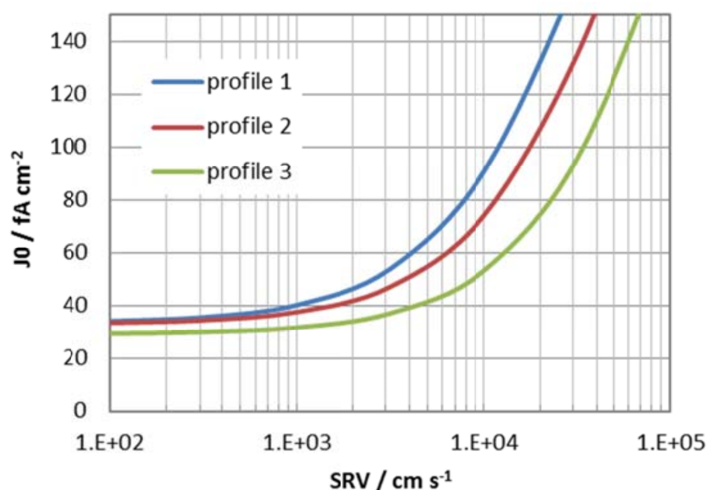

Figure 3: Calculated J_{0E} values for the different boron emitters as function of SRV.

3 Boron emitter improvements

3.1 Diffused boron emitter profiles

Standard diffused 60 ohm/sq boron emitters all exhibit a boron-depleted region in the first 10 – 30 nm of the profile. A typical boron emitter profile is shown in the blue line in figure 2, as profile 1. The depleted region originates from the higher solubility of boron in SiO_2 than in Si. SiO_2 is intentionally formed after boron-diffusion. This is necessary to reliably remove the boron-rich layer (BRL), a Si-B compound which is otherwise hard to remove and is detrimental for surface passivation [17]. In our improved emitter process, we etch this boron-depleted region by 10-20 nm with negligible damage to the surface texture. Our patented technology of chemical oxide passivation process [18] does not re-introduce boron depletion due to its low process temperature. The resulting boron emitter profile will then look as profile 2 or 3 in figure 2, depending on the etch depth.

Conventionally it is assumed that a higher surface concentration increases the defect density at the surface, and therefore results in a poorer surface passivation. However, this conventional assumption does not take into account the more favorable (lower) surface concentration of minority carriers that can be

achieved with a higher surface doping. The lower minority carrier concentration at the surface results in a lower surface recombination rate, which in turn leads to the lower calculated J_{0E} values for profile 2 compared to profile 1. As can be seen from figure 3, even with a surface passivation scheme that results in SRVs of around 10^4 cm/s for 'standard' n-Pasha cells, the J_{0E} value decreases from 100 fA/cm^2 to 70/55 fA/cm^2 when going from emitter profile 1 to 2/3.

3.2 Experimental results on improved emitters

Figure 4 shows the implied V_{oc} data obtained with symmetrically diffused lifetime samples with emitter profiles 1, 2 and 3. The surface pretreatment and passivation schemes were in all cases according to our 'n-Pasha baseline' standard. The observed gain in implied V_{oc} of 12 mV for profile 1→ 2 corresponds to a decrease in J_0 of the sample by 100 fA/cm^2, i.e. 50 fA/cm^2 for J_{0E} on each side. For profile 3, even higher values for implied V_{oc} and lower J_{0E} are obtained. These J_{0E} values are consistent with SRV values of 5000-10000 cm/s in Figure 3 for all profiles. Moreover, this strongly suggests that the lower boron surface concentration in the boron depletion layer does not reduce the surface recombination rate.

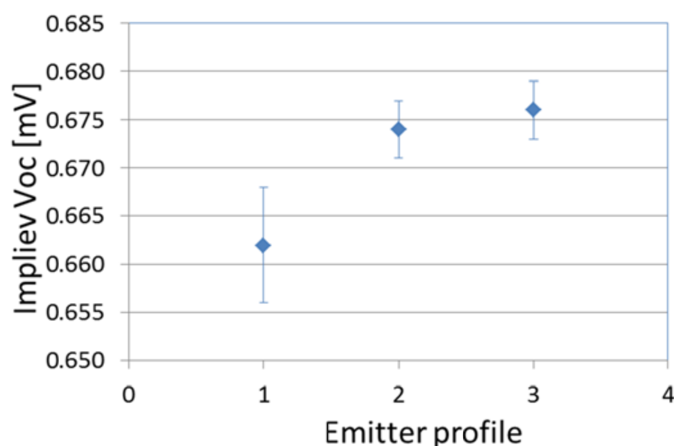

Figure 4: Implied V_{oc} for the symmetrically diffused lifetime samples with emitter profiles 1, 2 and 3 from Figure 2.

The beneficiary effect of reducing the boron depleted region is confirmed by cell results. In this initial test on cell level, only profile 1 and 2 are compared, both with an R_{sheet} of 60 ohm/sq. The V_{oc} increase of ~ 6 mV of n-Pasha cells is in agreement with the J_{0E} reduction of ~50 fA/cm^2, resulting in an efficiency gain of ~ 0.2% absolute, as can be seen in Table 1.

Table 1: Average IV results for emitters with profiles 1 and 2

		I_{sc} [A]	J_{sc} [mA/cm^2]	V_{oc} [V]	FF [-]	eta [%]
1: Standard 60 ohm/sq	avg	9.31	39.0	0.646	0.784	19.7
2: Improved 60 ohm/sq	avg	9.35	39.1	0.652	0.779	19.9

To enable even higher efficiencies, emitter profile 3 can be appropriate. However, this emitter has a higher sheet resistance, and the front side metallization pitch will need to be adjusted for optimal efficiency.

4 Surface passivation improvements

4.1 Improved chemical pretreatment

The next step for front side improvement is to reduce the surface recombination velocity (SRV) further. This is achieved by improving both the chemical pretreatment (originally a standard HF dip), the chemical oxide treatment itself and subsequently applying an ALD Al_2O_3 coating. For all initial tests, the emitter is kept the same, the 'standard' profile 1. Improving the chemical pretreatment alone already resulted in a gain in cell efficiency of 0.3% absolute, as can be seen in table 2. This gain if primarily due to an improved V_{oc} by 6 mV, indicating an improved surface passivation. Furthermore, there is an improvement in FF, related to an improved diode behavior. This is also reflected in a significant decrease in diode factor n from 1.42 to 1.27.

Table 2: IV results for improved oxide pretreatment versus standard HF dip

		I_{sc} (A)	J_{sc} (mA/cm2)	V_{oc} (V)	FF (-)	n	eta (%)
Standard HF dip	avg	9.31	39.0	0.649	0.785	1.42	19.8
Improved pretreatment	avg	9.30	38.9	0.655	0.788	1.27	20.1

4.2 Al_2O_3 passivation

To achieve optimal passivation, combinations of the other parameters were tested on n-Pasha half fabricates while the improved chemical pretreatment was used for all samples. The experimental groups used in this test are listed in table 3. All groups consisted out of 3 – 5 n-Pasha cells processed up to metallization. To activate the passivation, the samples all received a high temperature anneal in the form of the standard n-Pasha firing step.

Table 3: Sample description of the passivation Design of Experiments

Parameters	G1	G2	G3	G4	G5	G6
Oxidation method	A	A	A	NAOS	NAOS	NAOS
Oxidation time	Short	Short	Long	Short	Long	Long
Al_2O_3	no	yes	yes	yes	No	yes

The resulting values for implied V_{oc} are shown in Figure 5. As can be seen, a combination of a NAOS oxidation with Al_2O_3 passivation (group 6) resulted in the best passivation, with an average implied V_{oc} of 676 mV. Highest implied V_{oc} values of 682 mV were reached with this passivation method.

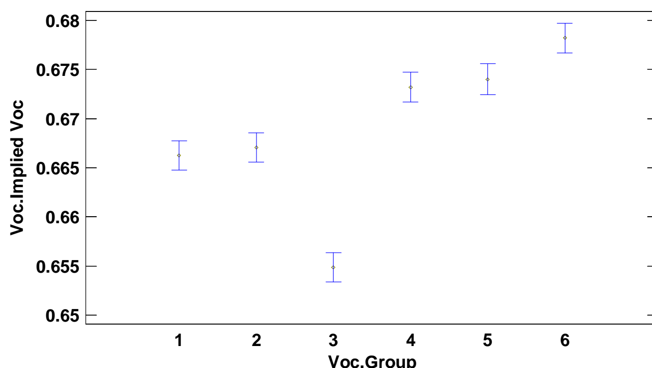

Figure 5: Implied V_{oc} measurements as a function of the groups (means and 95 percent LSD intervals)

In Figure 6, both subsequent improvements of the passivation (wet chemical pretreatment and Al_2O_3 passivation) are shown, each step increasing the lifetime (shown as implied V_{oc} in Figure 6a), reducing J_0 (not shown) and SRV (Figure 6b). The SRV is estimated based on the Atlas simulations of the standard boron profile nr 1 (see Figure 2). The lifetime samples used here were again n-Pasha half fabricates, made with an emitter on one side and a BSF on the other. An increase of the implied V_{oc} from 664 mV for our 'standard n-Pasha' towards 676 mV for the 'optimally passivated n-Pasha' corresponds to a decrease in J_{0E} by ~70 fA/cm^2, e.g from ~ 110 fA/cm^2 down to ~ 40 fA/cm^2 which in turn corresponds to a decrease in SRV of almost 1 order of magnitude from above 10000 cm/s to about 1000 cm/s. At an SRV value of 1000 cm/s the J_{0E} of the emitter is determined by the Auger recombination, which means that the surface passivation is not the limiting factor anymore.

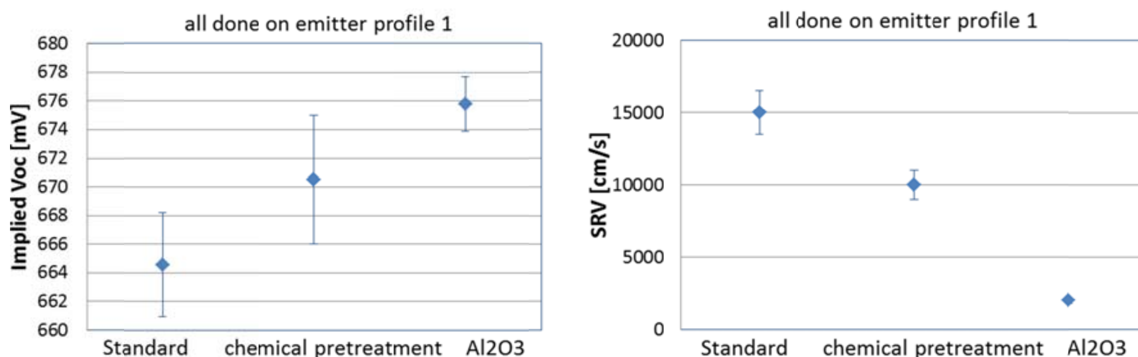

Figure 6: Implied V_{oc} (a) and SRV values (b) for the subsequent improvements for surface passivation

5 Implementation on cell level

The current n-Pasha baseline process typically has an average efficiency of 20.0-20.1%, relies on the emitter profile 1 and passivation schemes as in the reference groups. A recent cell run, implementing the improved chemical pretreatment into our n-Pasha baseline resulted in average efficiencies of 20.4% with a highest efficiency of 20.5%.

Table 4: IV results for standard n-Pasha 'baseline' solar cells

	Isc (A)	Jsc (mA/cm2)	Voc (V)	FF (-)	eta (%)
Avg (24 cells)	9.50	39.73	0.654	0.785	20.4
top	9.52	39.85	0.656	0.788	20.5

The improvements for emitter and Al_2O_3 passivation as explained above are planned to be implemented in the coming month. Only implementing emitter profile 2 resulted in a gain of conversion efficiency of 0.2% absolute, and adding Al_2O_3 surface passivation a gain in V_{oc} of ~10 mV, and an efficiency gain of 0.4% absolute is expected which should bring the n-Pasha cell efficiency close to 21%. It must be noted however, that the efficiency gains related to modified profiles and improved passivation are not always additive. Ultimately, the choice of the best combination will be made considering the CoO and process simplicity and process control.

6 Summary

Recombination within the boron diffused emitter region and on its surface limits the efficiency of n-Pasha solar cells. In this paper, we have shown several industrially feasible routes to reduce the recombination at the front side. First of all, we presented a simple and effective method to tune the emitter profile such that the recombination is decreased while the sheet conductance and contact ability is largely unaffected. The emitter recombination current J_{0E} is decreased from 110 fA/cm^2 to 60 fA/cm^2 while maintaining the sheet resistance at 60 ohm/sq. n-Pasha cells made with these profiles exhibit a higher V_{oc} by 6 mV and a higher efficiency by 0.2% absolute. Furthermore, several parameters related to the surface cleaning, variations of chemical oxide passivation and dielectric layers have also been investigated. We found that a very high implied V_{oc} of 680±2 mV can be obtained with an improved pre-cleaning followed by a wet chemical surface oxidation and ALD Al_2O_3 capped with PECVD-SiN_x. The associated values for SRV are reduced from above 10^4 cm/s towards 1000 cm/s. Combining the improved emitter profile and the improved surface passivation, values of J_{0E} of 40 – 50 fA/cm^2 for contactable boron emitters are within reach The novel chemical pretreatment alone already shows improvements of the n-Pasha cell efficiency of 0.3% absolute when combined with the standard passivation by NAOS/SiN_x

n-Pasha cells with 'baseline' processing including the new chemical pretreatment now result in efficiencies up to 20.5%. Further implementation of the emitter modifications and passivation schemes described in this paper is expected to result in a large step towards efficiencies of 21%.

References

[1] G.J.M. Janssen, et al., EU PVSEC, Paris, 2013

[2] SEMI PV Group Europe 2013, International technology roadmap for photovoltaic (ITRPV): Results 2012, 4th edn. (March).

[3] S. Glunz et al. 1998, Proc. 2nd WCPEC, Vienna, Austria, p. 1343.

[4] D. Macdonald & L.J. Geerligs, 2008, Appl. Phys. Lett., vol 92, p. 4061

[5] P. Cousins et al., 2010, 36th IEEE PVSC, Hawaii, USA

[6] T. Mishima et al., 2011, Solar Energy Mater. & Solar Cells 95, p18-21

[7] D. Song et al., 2012, Proc. 38th IEEE PVSC, Austin, USA

[8] A.R. Burgers et al., 2011, Proc. 26th EUPVSEC, Hamburg, Germany

[9] I.G. Romijn et al., 2013, Photovoltaics International, 20th edn, p33

[10] I.G. Romijn et al., 2013, Proc 28th EUPVSEC, Paris, France

[11] I.G. Romijn et al., 2012, Proc. 27th EUPVSEC, Frankfurt, Germany

[12] N. Guillevin et al., 2014, "High efficiency n-type MWT cells and modules using industrial processes", this conference, Shanghai, China

[13] A. Burgers et al., 2014, Mercury IBC cells, this conference, Shanghai, China

[14] N. Guillevin et al., Proc. 27th EU-PVSEC, Hamburg, Germany

[15] I. Cesar et al., "Mercury: a BJBC with novel design for high efficiency an simplified processing", Energy Procedia, 4th Int. Conf. on Silicon Photovoltaics, Den Bosch, the Netherlands

[16] Atlas from Silvaco Inc. Santa Clara, CA, www.silvaco.com.

[17] A.H.G. Vlooswijk, et al., 'Boron processing in solar cell industry : Boron diffusion in silicon wafers' Chapter 16, 'Boron: Compounds, Production and Application', Nova Science Publishers, 2010

[18] Y. Komatsu, L.J. Geerligs, and V.D. Mihailetchi WO2008/039067, or V.D. Mihailetchi, et al., Appl. Phys. Lett. 92, 063510 (2008).